ACS OMEGA

Open Access

http://pubs.acs.org/journal/acsodf

Article

DFT Insights into MAX Phase Borides Hf_2AB [A = S, Se, Te] in Comparison with MAX Phase Carbides Hf_2AC [A = S, Se, Te]

Jakiul Islam, Md. Didarul Islam, Md. Ashraf Ali,* Hasina Akter, Aslam Hossain, Mautushi Biswas, Md. Mukter Hossain, Md. Mohi Uddin, and Saleh Hasan Naqib*

Cite This: *ACS Omega* 2023, 8, 32917−32930

Read Online

ACCESS | Metrics & More | Article Recommendations | Supporting Information

ABSTRACT: In this work, density functional theory (DFT)-based calculations were performed to compute the physical properties (structural stability, mechanical behavior, and electronic, thermodynamic, and optical properties) of synthesized MAX phases Hf_2SB, Hf_2SC, Hf_2SeB, Hf_2SeC, and Hf_2TeB and the as-yet-undiscovered MAX carbide phase Hf_2TeC. Calculations of formation energy, phonon dispersion curves, and elastic constants confirmed the stability of the aforementioned compounds, including the predicted Hf_2TeC. The obtained values of lattice parameters, elastic constants, and elastic moduli of Hf_2SB, Hf_2SC, Hf_2SeB, Hf_2SeC, and Hf_2TeB showed fair agreement with earlier studies, whereas the values of the aforementioned parameters for the predicted Hf_2TeC exhibit a good consequence of B replacement by C. The anisotropic mechanical properties are exhibited by the considered MAX phases. The metallic nature and its anisotropic behavior were revealed by the electronic band structure and density of states. The analysis of the thermal properties—Debye temperature, melting temperature, minimum thermal conductivity, and Grüneisen parameter—confirmed that the carbide phases were more suited than the boride phases considered herein. The MAX phase's response to incoming photons further demonstrated that they were metallic. Their suitability for use as coating materials to prevent solar heating was demonstrated by the reflectivity spectra. Additionally, this study demonstrated the impact of B replacing C in the MAX phases.

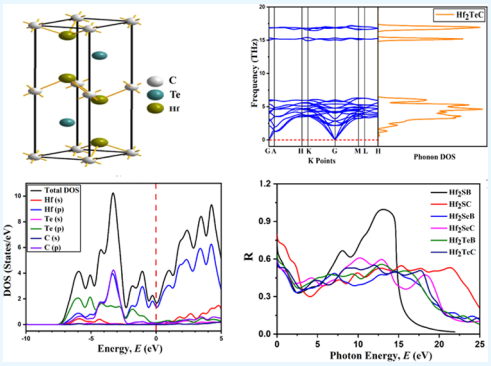

1. INTRODUCTION

One of the most thoroughly investigated groups of transition-metal borides, carbides, or nitrides is denoted by the notation $M_{n+1}AX_n$, where M is any of the transition-metal elements, A is an A-group element selected from columns 13−16 of the periodic table, and X denotes boron, carbon, or nitrogen.[1,2] The properties of metals and ceramics are combined in MAX phase materials, which are exceptionally resistant to oxidation and corrosion, elastically rigid, have higher melting temperature, and are lightweight and machinable. They also have excellent electrical and thermal conductivity, are resistant to thermal shock, and have plasticity at high temperatures. They can therefore be utilized as a substitute for both ceramic and metal depending on the application. MAX phase materials have recently been used for various technological and industrial purposes, including in the nuclear industry and high-temperature applications, electric circuits, sensors, heat exchangers, metal-refining electrodes, and aerospace.[3−7] Researchers and engineers are encouraged to theoretically or experimentally explore the MAX phase compounds because of their appealing features. Till now, more than 150 MAX phases made up of 32 elements have been identified.[1,8]

The combination of the strong covalent M−X bond and the weak metallic M−A bond is responsible for the combined characteristics (metal and ceramic) of MAX phases. The element and composition of M, A, and X (M = Ti, V, Cr, Ta, Zr, Hf, Nb, and so on; A = Al, S, Se, Sn, As, In, Ga; and X = N, C) can readily be changed, which allows for easy modification of the MAX phase's physical and chemical characteristics. Especially, the substitution of the M and A sites is the best choice for the prediction of new MAX phases, such as (Sc, Ti, Cr, Zr, Nb, Mo, Hf, Ta)$_2$AlC,[9] (Ti, V, Nb, Zr, Hf)$_2$SnC,[10,11] (Ti, Zr, Hf)$_2$SC,[12,13] (Zr, Hf, Nb)$_2$SC,[14] V_2(Al, Ga)C,[2,15,16] Ti_2(Zn, Al, In, Ga)C,[17] and Cr_2(Al, Ge)C.[18] A mixture of A-site elements also demonstrated a synergistic impact of both atoms (increased physicochemical properties) were also shown in a number of investigations. For instance, Li et al. synthesized a series of $V_2(A_xSn_{1-x})C$ phases (A = Fe, Co, Ni, Mn, or their mixture).[19] They investigated the impact of alloying A-site elements on the magnetic properties.[19] However, the majority of the variation in the X site was restricted to either carbon or

Received: June 21, 2023
Accepted: August 16, 2023
Published: August 29, 2023

nitrogen or a combination of the two.[14] Boron has recently been added to this list.[20] Rackl et al. have recently synthesized and studied the crystal structure, stability, chemical bonds, and elastic and electronic properties of prepared Zr_2SB and Hf_2SB MAX phase borides for the first time.[20] The prepared Hf_2SB MAX phase exhibits metallic character and Pauli paramagnetism. Additionally, density functional theory (DFT) calculations show that the ionic bonds are somewhat weaker than those of carbides, resulting in lower bulk moduli of this boride than for the comparable carbide.[21] In another literature, the mechanical properties, elastic anisotropy, optical properties, dynamic stability, and thermal properties of Hf_2SB and Hf_2SC were investigated.[14] Wang et al.[22] synthesized Hf_2SeC and compared it with Hf_2SC; due to a longer bonding length of Hf−Se than Hf−S, a lower bonding energy and a softer structure of Hf_2SeC are expected, which results in a larger thermal expansion coefficient (TEC) of Hf_2SeC than that of Hf_2SC. Similar results were also observed for Zr_2SeC and Zr_2SC.[22] Zhang et al. theorized the stability and lattice characteristics of the Hf_2SeB MAX phase in a different work, in which successful synthesis of this compound using the thermal explosion method in a spark plasma sintering furnace was reported.[23] Recently, Zr_2SeB and Hf_2SeB, two MAX phases that were both thermodynamically and mechanically stable, were predicted by Zhang et al.[24] They also synthesized these phases by thermal explosion technique in a spark plasma sintering furnace.

Since sulfur, selenium, and tellurium are in the same periodic table group with similar electronic structures, tellurium is also expected to be a potential A-site element of the ternary carbides and/or borides belonging to the MAX phase family. Zhang et al. brought the B-Te chemistry to light by synthesizing the first tellurium (Te)-containing layered ternary compound Hf_2TeB using the thermal explosion method.[25] The dynamical stability and mechanical properties of Hf_2TeB have also been investigated by Zhou et al.[26] Since the Hf_2TeB MAX phase has yet to be completely investigated, more theoretical data, such as elastic anisotropy indices, thermodynamical properties, and optical properties, should be scrutinized. Knowledge of mechanical properties is important for structural materials, but the lack of information regarding mechanical anisotropy may restrict their use, as it (anisotropy) is related to direction-dependent plastic deformation, fracture propagation, and elastic instability. On the other hand, the Vickers hardness measures the ultimate mechanical strength of solids, which is a pre-requisite for application in any structural component. The ultimate use of MAX phase materials in high-temperature environments (such as thermal barrier coating materials) depends on the values of thermophysical parameters (Debye temperature, minimum thermal conductivity, melting temperature, Grüneisen parameter, etc.) that characterize the thermal properties of solids. The use of MAX phase materials in spaceships as coating materials to reduce solar heating depends on the value of the optical reflectivity. Thus, the study of thermal and optical properties is scientifically important to broaden the scope of Hf_2TeB for potential uses. Motivated by the synthesis of Hf_2TeB and based on our accumulated knowledge about the MAX phase chemistry, we assumed that Hf_2TeC might be a potential member of the MAX phase family. Consequently, we investigated the stability of Hf_2TeC for the first time by calculating the formation energy, phonon dispersion curve (dynamical stability), and elastic constants (mechanical stability). The aforementioned physical properties of Hf_2TeC, as a new member of MAX phase materials, should also be explored to disclose its potential in various sectors of application. In addition, the effect of A-element replacing on the physical properties might be an interesting topic of MAX phases; consequently, the inclusion of the properties of previously studied MAX phases, Hf_2SB,[20] Hf_2SC,[27] Hf_2SeB,[23] and Hf_2SeC,[22,27] is also scientifically important.

Therefore, we aimed to perform a DFT-based study for the synthesized Hf_2SC, Hf_2SB, Hf_2SeC, Hf_2SeB, and Hf_2TeB and newly predicted Hf_2TeC. Hence, the structural, mechanical (including Vickers hardness and elastic anisotropy), electronic, thermal, and optical properties of Hf_2AX [A = S, Se, Te; X = C, B] MAX phase compounds have been presented in this article.

2. COMPUTATIONAL METHODS

The scientific community in the areas of physics and materials engineering has shown a significant deal of interest in computer-based ab initio calculations utilizing the DFT.[28,29] The Cambridge Serial Total Energy Package (CASTEP)[30] code, which is based on the DFT, was used for the crystal geometry computations and characteristics analysis in the current study of MAX phases. The generalized gradient approximation (GGA), along with Perdew−Burke−Ernzerhof (PBE),[31] was used to describe the exchange−correlation energy. The ultrasoft pseudopotential suggested by Vanderbilt[32] was chosen for calculating the electron−ion interaction. Ultrasoft pseudopotentials (USP) were introduced by Vanderbilt in 1990. The USP offers a possibility to resolve the problem of plane-wave convergence for transition metals with good accuracy. In USP, the norm-conservation constraint is relaxed and the difference in the charge densities calculated from the all-electron and pseudo-orbitals is described in terms of a small number of localized augmentation functions. This allows calculations to be performed with the lowest possible cutoff energy for the plane-wave basis set. The Broyden−Fletcher−Goldfarb−Shanno (BFGS) scheme[33] was used to ensure geometry optimization. The pseudo-atomic calculations were performed, taking only valence electrons to reduce the core-electron effects. The crystal geometry was optimized and the physical properties were calculated using a *k*-point mesh of size 10 × 10 × 3 (Monkhorst−Pack schemes)[34] and a cutoff energy of 500 eV. The convergence criteria were selected as follows: total energy: 5×10^{-6} eV/atom; maximum force: 0.01 eV/Å; maximum ionic displacement: 5×10^{-4} Å; and maximum stress: 0.02 GPa.

3. RESULTS AND DISCUSSION

3.1. Structural Properties and Stability. Figure 1 depicts the crystal structure of ternary Hf_2SB MAX phases that crystallize to a hexagonal structure [space group *P*6$_3$*mmc*] just like the other C- or N-containing MAX compounds.[14,20−22,24,26,27,35] The investigated MAX phase compounds have two formula units, each of which has four atoms. The atomic positions of these MAX phase compounds are as follows: Hf atoms at 4f (0.3333, 0.6667, Z_M), A atoms at 2d (0.3333, 0.6667, 0.75), and X atoms at 2a (0, 0, 0) sites. The other crystallographic data of Hf_2SB (as a representative) are presented in the Supporting document.

The DFT-optimized lattice constants (*a*, *c*), *c*/*a* ratios, and internal parameters (z_M) of the studied MAX boride and carbide phases are listed in Table 1, together with other available theoretical and experimental results. These DFT-

https://doi.org/10.1021/acsomega.3c04283
ACS Omega 2023, 8, 32917−32930

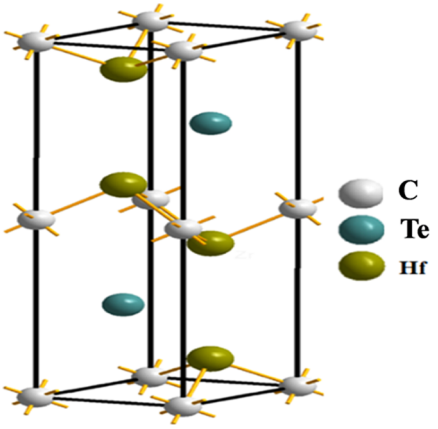

Figure 1. Crystal structure of the Hf_2TeC compound.

optimized lattice constants (a and c) show good consistency with earlier experimental as well as theoretical studies, as can be shown in Table 1. Lattice constant c of the Hf_2TeB phase is determined to have a maximum divergence from the experimental value of 1.74%. These agreements suggest that the current investigation is highly reliable. The Hf_2TeC MAX phase is predicted for the first time; as a result, it was not possible to make a comparison with other previous reports for this particular carbide. This DFT-predicted result for Hf_2TeC can be a useful reference work for designing future experimental as well as theoretical research works.

The phonon dispersion curve (PDC) can be used to analyze a compound's dynamic stability, vibrational contribution to the energy, and various phonon modes.[36−39] As most of the MAX phases are synthesized at a higher thermal treatment (at a higher temperature), those materials may not be stable under all conditions. In order to check the dynamic stability of Hf_2TeX (X = B,C), phonon dispersion curves (PDCs) have been calculated using the density functional perturbation theory (DFPT) within the linear-response method.[14,40] The calculated phonon dispersion curves (PDCs) and total phonon density of states (PHDOS) of individual MAX phase compounds along the high-symmetry paths of the Brillouin zone (BZ) are displayed in Figure 2. The presence of only positive frequencies indicates the dynamical stability of the compound. As there are no negative frequencies detected in the PDCs of Hf_2TeC, as displayed in Figure 2e, this MAX phase compound is predicted to be dynamically stable like its boride counterpart Hf_2TeB (PDCs presented in Figure 2f). Dynamical stability is also observed for the other MAX phases and are presented in Figure 2a−d.

To further aid in comprehending the bands, the PHDOS of Hf_2TeB and Hf_2TeC are shown beside the PDCs. Figure 2 shows that all of the MAX phase carbides have a distinct gap between their transverse optical (TO) and longitudinal optical (LO) frequencies, but no gaps are evident for the MAX phase borides. The separation between LO (top) and TO (bottom) modes at the central G point is 2.2, 1.6, and 1.6 THz for Hf_2SC, Hf_2SeC, and Hf_2TeC, respectively. Furthermore, for all of the MAX phases including carbides and borides, there is no phononic bandgap between the acoustic and low-energy optical phonon modes, but there is a pronounced phononic bandgap between high-energy and low-energy optical modes. Most importantly, at the Brillouin zone-center point (G) of the PDCs, the frequency of acoustic modes is zero in all of the MAX phases under study, which is another indication of the structural stability of the MAX phases under consideration.

The lattice dynamics of crystal is especially fascinating in terms of zone-center phonon modes. The 8 atoms that make up the 211 MAX phases give them a total of 24 phonon branches or vibration modes. There are 21 optical modes, and the remaining three are zero-frequency acoustic modes at the Γ-point. Six of these 21 optical modes are IR-active, seven are Raman-active, and the other eight are silent modes. The optical phonon modes with a Brillouin zone center can be expressed by the following groups:

Table 1. Calculated Lattice Parameters (a and c), Internal Parameter (z_M), c/a Ratio, and Formation Energy of Hf_2AX [A = S, Se, Te; X = B, C] MAX Phase Compounds

phase	a (Å)	% of deviation	c (Å)	% of deviation	z_M	c/a	E_F (eV/atom)	references
Hf_2SB	3.506	1.13	12.229	1.03	0.603	3.487	−1.26	this study
	3.467		12.104		0.604	3.491		expt.[20]
	3.482	0.43	12.137	0.27	0.603	3.485		theo.[20]
	3.506	1.13	12.159	0.45	0.603	3.468		theo.[14]
	3.508	1.20	12.222	0.97	0.603	3.483		theo.[26]
Hf_2SC	3.300	2.0	11.757	2.1	0.099	3.562	−1.13	this study
	3.369		12.017		0.600	3.566		expt.[20]
	3.360		11.997			3.570		expt.[21]
	3.424	1.63	12.184	1.39	0.600	3.558		theo.[14]
	3.369	0.01	11.993	0.19	0.101	3.560		theo.[22]
Hf_2SeB	3.552	0.85	12.559		0.099	3.535	−1.16	this study
	3.522		12.478		0.598	3.542		expt.[26]
	3.550	0.79	12.573		0.599	3.541		theo.[26]
Hf_2SeC	3.470	1.42	12.514	0.99	0.095	3.605	−1.03	this study
	3.422		12.391			3.621		expt.[24]
	3.436	0.41	12.452	0.49		3.624		theo.[24]
	3.438	0.47	12.501	0.89		3.636		theo.[27]
Hf_2TeB	3.629	0.68	13.355	1.74	0.591	3.679	−0.86	this study
	3.604		13.126			3.641		expt.[35]
Hf_2TeC	3.559		13.236		0.088	3.718	−0.69	this study

https://doi.org/10.1021/acsomega.3c04283
ACS Omega 2023, 8, 32917−32930

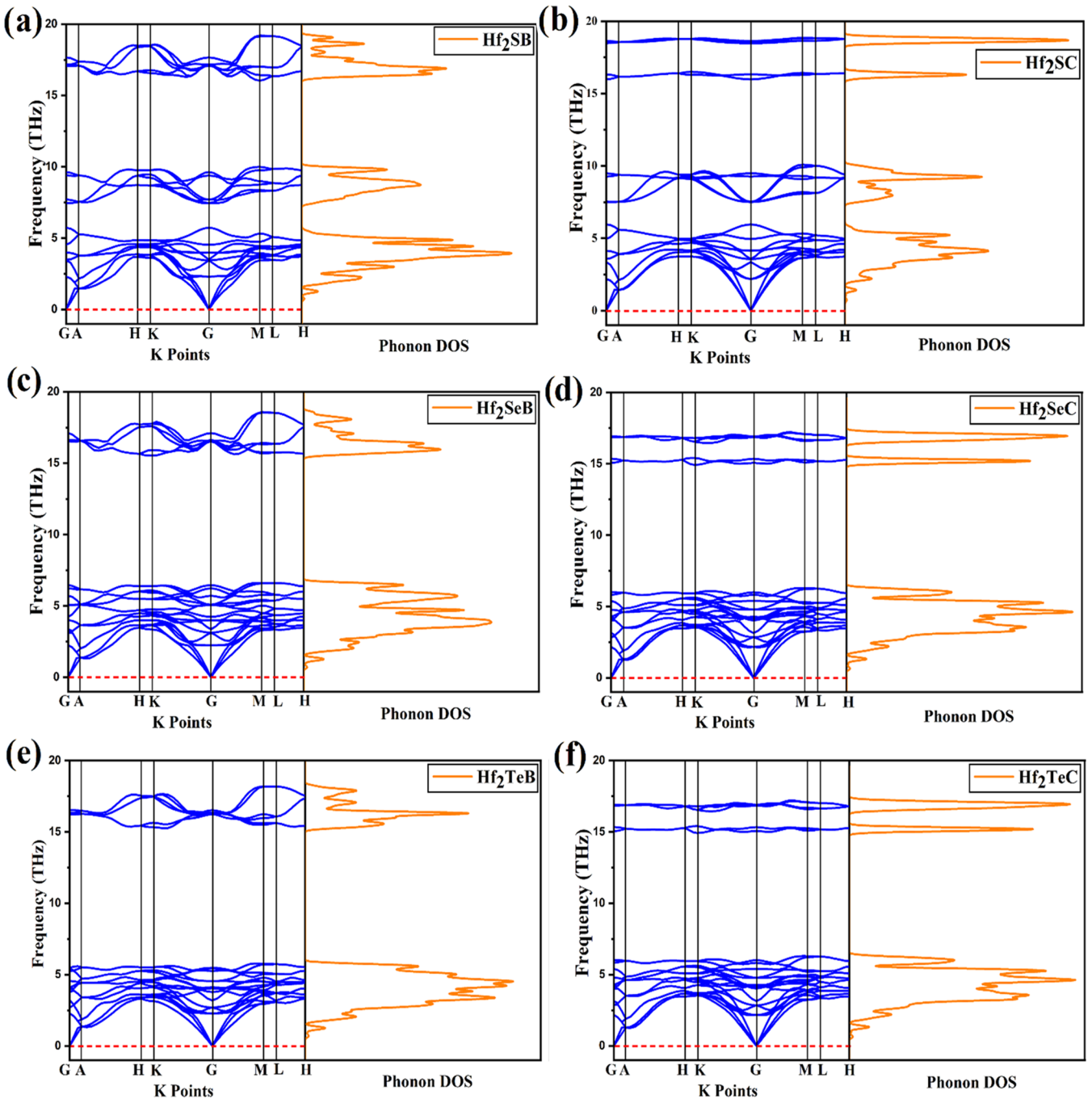

Figure 2. PDCs and PHDOS of (a) Hf_2SB, (b) Hf_2SC, (c) Hf_2SeB, (d) Hf_2SeC, (e) Hf_2TeB, and (f) Hf_2TeC compounds. The dashed line (red) is at zero phonon frequency.

$$\Gamma_{opt.} = 2A_{2u} + 4E_{1u} + 2E_{1g} + 4E_{2g} + A_{1g} + 2B_{1u} + 2B_{2g} + 4E_{2u}$$

where IR-active modes are A_{2u} and E_{1u}, Raman-active modes are A_{1g}, E_{1g}, and E_{2g}, and silent modes are B_{1u}, B_{2g}, and E_{2u}.[41,42]

The obtained modes for the Hf_2AX [A = S, Se, Te; X = C, B] phases in this study are in agreement with earlier theoretical investigations of the different 211 MAX phases. A specific vibrational frequency corresponds to each mode. Degenerate modes are those that occasionally have two or more modes with the same frequency but cannot be distinguished from one another. For this reason, Table S4 contains six IR-active modes and seven Raman-active modes for each phase.

3.1.1. Mechanical Properties. It is essential to study the elastic properties of a material to understand its mechanical behaviors, such as mechanical stability, ductility/brittleness, hardness, and machinability. The elastic constants (C_{ij}) are key parameters in figuring out the mechanical properties of solids. Because they are connected to various solid-state phenomena, including inter-atomic bonding and phonon spectra, elastic constants of solids are very important. Elastic constants are also related to the Debye temperature, thermal expansion, and specific heat from a thermodynamic perspective. Therefore, before moving on to a material's applications, it is highly

https://doi.org/10.1021/acsomega.3c04283
ACS Omega 2023, 8, 32917−32930

Table 2. Calculated Stiffness Constants (C_{ij}), Bulk Modulus (B), Machinability Index (B/C_{44}), Cauchy Pressure (CP), Shear Modulus (G), Young's Modulus (Y), Poisson's Ratio (ν), and Pugh Ratio (G/B) of Hf_2AX [A = S, Se, Te; X = B, C] MAX Phase Compounds

parameters	Hf_2SB	Hf_2SC	Hf_2SeB	Hf_2SeC	Hf_2TeB	Hf_2TeC
C_{11}(GPa)	285	350	232	287	182	257
	286[a]	344[d]	243[f]	308[e]	206[c]	
	285[b]	311[b]	244[c]	287[g]		
	265[c]	330[e]				
C_{33}(GPa)	298	371	274	305	243	277
	296[a]	369[d]	281[f]	314[e]	232[c]	
	298[b]	327[b]	281[c]	306[g]		
	305[c]	345[e]				
C_{44}(GPa)	130	176	120	130	107	112
	122[a]	175[d]	119[f]	135[e]	107[c]	
	130[b]	149[b]	119[c]	130[g]		
	125[c]	150[e]				
C_{12}(GPa)	81	98	98	77	77	81
	79[a]	116[d]	90[f]	93[e]	71[c]	
	81[b]	97[b]	90[c]	77[g]		
	100[c]	100[e]				
C_{13}(GPa)	92	118	88	97	83	92
	84a	138[d]	97[f]	105[e]	85[c]	
	92[b]	121[b]	87[c]	98[g]		
	90[c]	118[e]				
C_{55}(GPa)	130	176	120	130	107	112
C_{66}(GPa)	101	126	67[c]	104	52[c]	87
			79[f]			
B(GPa)	155	193	143	157	120	146
	151[a]	204[d]	144[f]	158[g]	125[c]	
	156[b]	181[b]	144[c]			
B/C_{44}	1.19	1.09	1.19	1.21	1.12	1.30
	1.23[a]	1.16[d]	1.21[f]	1.22[g]	1.17[c]	
	1.20[b]	1.21[b]	1.21[c]			
CP(GPa)	−49	−78	−22	−53	−30	−31
	−49[b]	−52[b]	−29	−53[g]	−36	
G(GPa)	111	142	89	112	73	97
	111[a]	134[d]	95[f]	113[g]	81[c]	
	112[b]	120[b]	95[c]			
Y(GPa)	268	344	222	273	183	238
	267[a]	330[d]	233[f]	273[g]	199[c]	
	270[b]	295[b]	233[c]			
ν	0.21	0.20	0.24	0.21	0.24	0.22
	0.20[a]	0.23[d]	0.23[f]	0.21[g]		
	0.21[b]	0.23[b]				
G/B	0.71	0.73	0.62	0.71	0.61	0.66
	0.73[a]	0.65[d]	0.66[f]	0.72[g]	0.65[c]	
	0.71[b]	0.66[b]	0.66[c]			

[a]Ref 20. [b]Ref 14. [c]Ref 26. [d]Ref 21. [e]Ref 22. [f]Ref 24. [g]Ref 27.

enlightening to look into its elastic properties. In this study, we have explored the detailed elastic properties of Hf_2TeB and Hf_2TeC. The elastic properties of Hf_2SB, Hf_2SC, Hf_2SeB, and Hf_2SeC have already been investigated earlier[14,20−22,24,26,27] and we have rechecked them also for further validation of our calculations. To the best of our knowledge, the elastic properties of Hf_2TeC have not yet been documented in any literature. Moreover, the layered ternary carbide phase Hf_2TeC is not yet synthesized. This study might be useful for designing and carrying out experimental and theoretical research on Hf_2TeC as well as other unexplored MAX phase compounds. The calculated elastic properties with previous reports are listed in Table 2. The hexagonal system possesses five independent elastic constants; C_{11}, C_{33}, C_{44}, C_{12}, and C_{13}. For a hexagonal system, the compound is said to be mechanically stable if it satisfies the stability conditions as presented by eq S2.

From Table 2, it can be observed that the studied MAX phase compounds are mechanically stable. This study provides the first demonstration of the mechanical stability of the Hf_2TeB and Hf_2TeC MAX phases using elastic constants. This prediction can be helpful for the experimental synthesis of unexplored ternary carbide MAX phase Hf_2TeC. Moreover, these elastic constants offer important details regarding stiffness in different directions. The elastic constants C_{11} and C_{33} depict the stiffness against applied stress along [100] and

https://doi.org/10.1021/acsomega.3c04283
ACS Omega 2023, 8, 32917−32930

Table 3. Calculated Mulliken Bond Number n^{μ}, Bond Length d_{μ}, Bond Overlap Population P^{μ}, Metallic Population $P^{\mu'}$, Bond Volume V_b^{μ}, and Bond Hardness H_v^{μ} of μ-type Bond and Vickers Hardness H_v of Hf_2AX [A = S, Se, Te; X = B, C] MAX Phase Compounds

compounds	bond	n^{μ}	d_{μ} (Å)	P^{μ}	$P^{\mu'}$	V_b^{μ} (Å^3)	H_v^{μ} (Gpa)	H_v (Gpa)
Hf_2SB	B−Hf	4	2.390	1.44	0.01497	13.331	14.07	7.746
	S−Hf	4	2.700	0.81		19.221	4.265	
Hf_2SC	C−Hf	4	2.236	1.26	0.00929	10.781	17.59	10.295
	S−Hf	4	2.600	0.92		16.949	6.025	
Hf_2SeB	B−Hf	4	2.403	1.76	0.014	34.323	3.563	3.563
Hf_2SeC	C−Hf	4	2.335	1.48	0.007	32.632	3.270	3.270
Hf_2TeB	B−Hf	4	2.4277	1.79	0.01502	38.0875	3.046	3.046
Hf_2TeC	C−Hf	4	2.363	1.51	0.00757	36.306	2.792	2.792

[001] directions, respectively. From Table 2, it is revealed that the value of $C_{33} > C_{11}$ for all of the studied MAX phases indicates that the *c*-axis has stronger deformation resistance than the *a*-axis. The fact that the value of C_{44} is less than C_{33} and C_{11} suggests that shear deformation is less difficult compared with that of axial deformation. The unequal values of C_{11}, C_{33}, and C_{44} ($C_{11} \neq C_{33} \neq C_{44}$) imply different atomic arrangements and hence different bonding strengths along the *a*-axis, *c*-axis, and shear planes. The elastic constants C_{12} and C_{13} have lesser values compared with the other three elastic constants. Additionally, C_{12} and C_{13} have smaller values compared with those of the other three elastic constants. The stiffness constants C_{12} and C_{13} indicate the applied stress toward the *a*-axis along with uniaxial strain along the *b*-, and *c*-axis, respectively. The C_{ij}s of Hf_2TeC are higher than those of Hf_2TeB. In comparison with other MAX phases, the C_{ij}s of Hf_2TeC are smaller than those of Hf_2SB, Hf_2SC, and Hf_2SeC, but higher than those of Hf_2SeB. However, with the exception of the C_{12} value for Hf_2SeB and Hf_2SeC, it is interesting to notice that the stiffness constant values of the carbide MAX phases are bigger than the corresponding boride MAX phases, indicating that the carbide phase is stiffer than its boride phase. Table 2 further shows that the stiffness constants in Hf_2SC are larger than those in other MAX phases, while those in Hf_2TeB are lower. This result suggests that among the studied compounds, Hf_2SC is the hardest MAX phase and Hf_2TeB is the softest MAX phase. The C_{ij} of the predicted phases, Hf_2TeC, should be compared with those of other Hf-based 211 carbides/borides. The $C_{11}\{C_{33}[C_{44}]\}$ found for Hf_2TeC is 257{277[112]} GPa, which is higher than those of Hf_2SeB [Table 2], Hf_2TeB [Table 2], Hf_2AlB [199 GPa],[9] Hf_2SiB [223 GPa],[43] and Hf_2PB [254 GPa].[43,44]

It is required to study the brittleness/ductility of material for a particular device application. The C_{ij} values help to predict the ductile/brittle behavior of a material. The Cauchy pressure (CP), which is defined as the difference between the elastic constant values C_{12} and C_{14}, is positive or negative depending on whether it represents the nature of ductility or brittleness.[14,45] The negative value of CP indicates the brittle behavior of the titled compounds. This result has been checked further by calculating the Pugh ratio and Poisson's ratio values using the computed elastic moduli.

The Voigt−Reuss−Hill (VRH) approximation schemes[46,47] are widely used to calculate the three different elastic moduli: bulk modulus (B), shear modulus (G), and Young's modulus (Y). The equations needed to calculate these elastic moduli are given in the supplementary file (eq S3).[1,48] The higher (lower) value of B and other elastic moduli implies the hard (soft) nature of a material.[24,49] From the tabulated values of B, G, and Y, it can be noticed that Hf_2TeC is harder than Hf_2TeB; in fact, Hf_2TeB is the softest one among tabulated compounds herein. Like stiffness constants, elastic moduli of Hf_2SC are also the largest, and Hf_2SC is harder compared with other MAX phase compounds. This result strongly supports the calculation of the stiffness constants.

The machinability index (μ_M),[50] is a useful parameter to predict the mechanical engineering performance of a material, which can be obtained by using the value of B and C_{44} with the formula, $\mu_M = \frac{B}{C_{44}}$. The higher (lower) value of μ_M signifies greater ease (difficulty) in making a desired shape of a solid. The μ_M of Hf_2TeC (1.30) is larger than that of Hf_2TeB (1.12). The stiffness constant and elastic moduli of Hf_2TeC are also larger compared with those of Hf_2TeB, confirming better suitability of Hf_2TeC than Hf_2TeB for tools applications. Among the considered phases, the highest value (1.30) of μ_M is observed for Hf_2TeC and the lowest value for Hf_2SC. The ductile/brittle behavior of the studied MAX phases has been investigated further using the Pugh ratio (G/B) and Poisson's ratio. The required equation to calculate the Poisson's ratio is expressed by eq S4. The critical value of the brittle/ductile boundary for the Pugh ratio (G/B) is 0.571,[51] and it is 0.26[52] for the Poisson's ratio (ν). The compound shows ductile (brittle) behavior, which possesses Pugh and Poisson's ratio values above (below) these critical values. The studied MAX phases are all brittle in nature, which has been also revealed from the CP calculation.

3.1.2. Mulliken Population Study. The atomic population analysis can be used to determine the charge transfer mechanism in a compound. As seen in Table S1, the negative charge of the atom indicates the electron receiver and the atom's positive charge indicates the electron donor during compound formation. In the case of Hf_2TeC and Hf_2TeB, Hf and Te atoms donate the charge to C and/or B atoms. Moreover, the charge is transferred from Hf to S and B/C for Hf_2SB and Hf_2SC MAX phases. Like Hf_2TeC and Hf_2TeB phases, both Hf and Se also exhibited positive charge indicating the electron donor nature of Hf and Se atoms for Hf_2SeC and Hf_2SeB phases. It can be confirmed from the periodic nature of the electronic configurations that the metallic nature is increased from top to bottom in the same series of periodic table atoms. The charge transfer mechanism also confirms the existence of ionic behavior of the MAX phases.

The Mulliken bond overlap population (BOP) indicates the bonding and antibonding nature of the individual bond in the compound by the positive and negative values, respectively. The BOP value of zero indicates no significant interaction

https://doi.org/10.1021/acsomega.3c04283
ACS Omega 2023, 8, 32917−32930

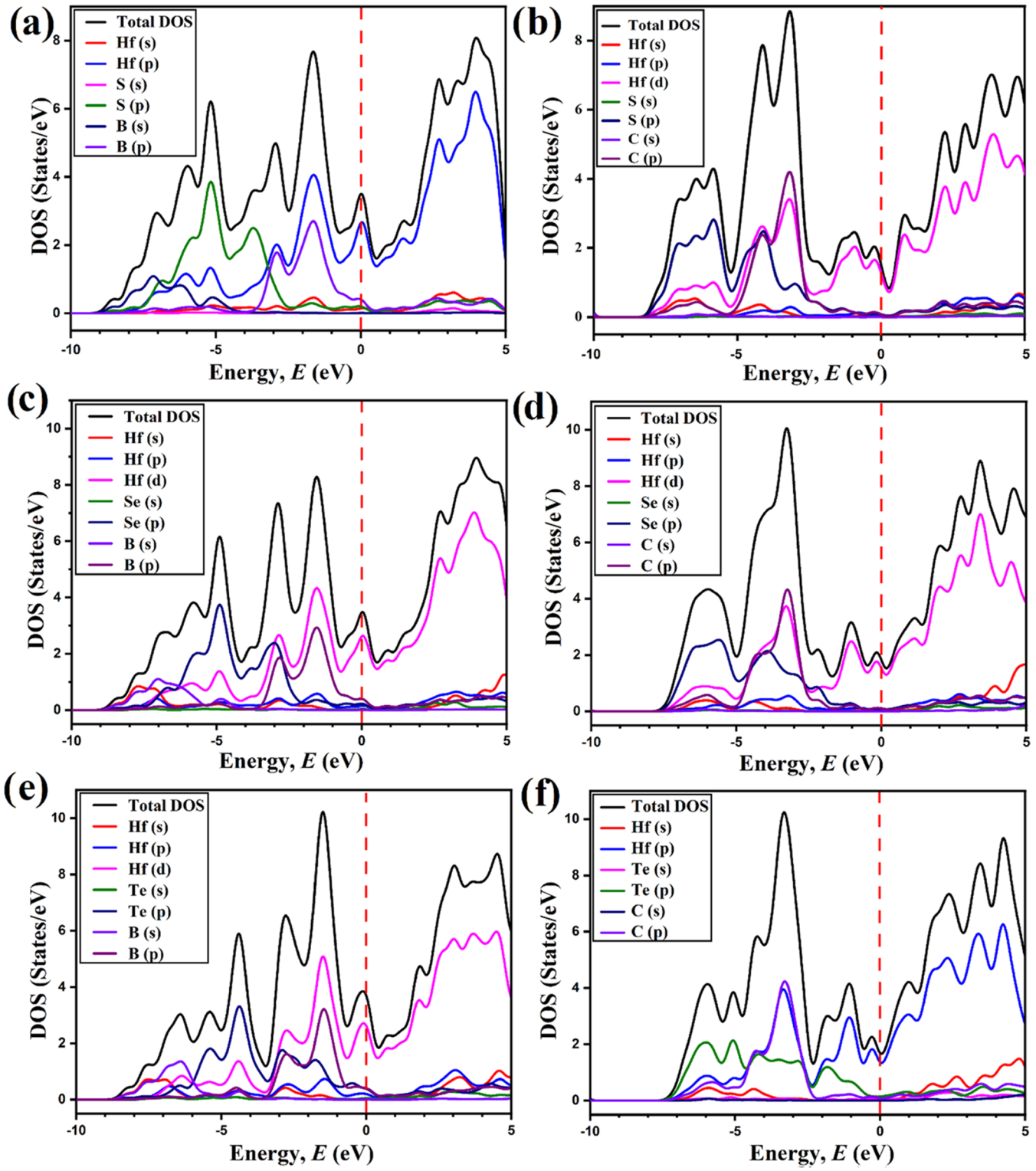

Figure 3. TDOS and partial density of states (PDOS) of (a) Hf_2SB, (b) Hf_2SC, (c) Hf_2SeB, (d) Hf_2SeC, (e) Hf_2TeB, and (f) Hf_2TeC compounds.

between the atoms involved in the bonding, while the higher value of BOP represents a higher degree of covalency of the bond. Table S2 shows a strong covalent bond between Hf−X (B, C) for all of the MAX phase compounds. Herein, it should be noted that the degree of covalency of the Hf−B bond is higher than that of the Hf−C bond, resulting in the higher bonding strength of the Hf−B bond. In conclusion, it can be predicted from the Mulliken population analysis that all of the MAX phases exhibited both ionic and covalent bonding nature.

3.1.3. Vickers Hardness. In Section 3.1.1, we have discussed several mechanical parameters including stiffness constants (C_{ij}), bulk modulus (B), shear modulus (G), and Young's modulus (Y) of individual MAX phase compounds. However, the intrinsic hardness of a material is completely different from those selected mechanical parameters though there may be a

https://doi.org/10.1021/acsomega.3c04283
ACS Omega 2023, 8, 32917−32930

correlation among them.[53] For this reason, in this study, we calculate the hardness (Vickers hardness, H_v) of all Hf_2AX [A = S, Se, Te; X = C, B] compounds using the formula given in eq S7. The obtained results from the calculations are summarized in Table 3.

From Table S2, the Mulliken bond overlap population confirmed that the Hf−X (X = B/C) covalent bonds are stronger than Hf−A (A = S/Se) in MAX phase compounds.[14] Moreover, it has been found from Table S2 that Hf−B bonds are stronger than Hf−C for all MAX phases, which is an indication of enhanced mechanical properties of MAX phase borides compared with the carbides.[36,53] The higher H_v of Hf_2TeB (3.05 GPa) compared with Hf_2TeC (2.79 GPa) supports the previous statement. Similarly, the Vickers hardness (Table 3) of Hf_2SeB is also higher compared with that of carbides, Hf_2SeC phase. The Vickers hardness of Hf_2SC, on the other hand, is higher than that of Hf_2SB. In this study, the calculated Vickers hardness values can be ranked as follows: Hf_2SC (10.30 GPa) ≥ Hf_2SB (7.75 GPa) ≥ Hf_2SeB (3.56 GPa) ≥ Hf_2SeC (3.27 GPa) ≥ Hf_2TeB (3.05 GPa) ≥ Hf_2TeC (2.79 GPa).

3.1.4. Elastic Anisotropy. Elastic anisotropy of a solid is important to study the direction-dependent bonding natures along different crystallographic directions. The knowledge of anisotropy indices provides significant information regarding possible microcracks under stress and unusual phonon modes. Therefore, a detailed exploration of anisotropy indices is required for practical applications of a material. The anisotropy factors of Hf_2SB and Hf_2SC have been investigated earlier.[14] The detailed anisotropy indices of Hf_2SeB, Hf_2SeC, Hf_2TeB, and Hf_2TeC are yet to be investigated. Considering this, we have calculated the various anisotropy factors of these MAX phases along different crystallographic directions and tabulated those in Table S3.

The three different shear anisotropy indices (A_1, A_2, and A_3) have been obtained using the well-known relations as presented in the supplementary file (eq S11). A value of A_i (i = 1, 2, 3) equal to 1 indicates an isotropic nature, otherwise anisotropic. The non-unit (1) values of A_i indicate the anisotropic behavior of the titled compounds. The bulk modulus anisotropy factors along the *a*- and *c*-axes, indicated as B_a and B_c, are found using the relations as presented in the supplementary file (eq S12).

The unequal values of B_a and B_c ($B_a \neq B_c$) indicate an anisotropic nature. The observed values of B_a and B_c for Hf_2SB and Hf_2SC show notable deviation from the previous study, though other anisotropy factors show good agreement.[14] The ratio of linear compressibility coefficients (k_c/k_a) is calculated using the relation given by eq S13.

The calculated values of k_c/k_a ratio listed in Table S3 deviate from unity, further ensuring the anisotropic nature of the studied MAX phases. The bulk modulus anisotropy factor (A_B) and the shear modulus factor anisotropy (A_G) are also estimated using eq S14. The universal anisotropic index (A^U) is another indicator that is taken into account while analyzing anisotropy. Equation S15 is used to get the A^U from the Voigt- and Reuss-approximated *B* and *G*.

The estimated values of A_B, A_G, and A^U are listed in Table S3. The nonzero values of A_B, A_G, and A^U notify the anisotropic nature of the studied MAX phases. From this study of different anisotropy factors, it can be concluded that all of the investigated MAX phase compounds are anisotropic in nature, and consequently their mechanical/elastic properties are also direction dependent.

3.2. Electronic Band Structure (EBS) and Density of States (DOS). The knowledge of the electronic band structure (EBS) of a compound is required to understand its optical and electronic transport properties. The energy band structures of the MAX phases are calculated along the high-symmetry points in the *k*-space directions such as G−A−H−K−G−M−L−H within the BZ and are depicted in Figure S1. The horizontal red dashed line at zero of the energy scales indicates the Fermi level (E_F). Figure S1 shows that the conduction and valance bands overlap at the E_F for the studied phases, indicating their metallic nature. The electronic band structure reveals anisotropic conductivity since the dispersion curves in the basal plane and *c*-direction differ significantly from one another. Similar anisotropic conductivity for other MAX phases has been also reported in previous studies.[21,27,54]

The total and partial density of states (DOS) is investigated to get a clear perception of the electronic properties of the MAX phases under investigation. From Figure 3, it is obvious that the total DOS at the E_F is finite, indicating the metallic feature of all of the MAX phases. Moreover, relative heights or the existence of a pseudo gap in the TDOS at E_F indicate the presence of a stable covalent bond (stability of MAX phases) within the crystal structure.[13] The obtained TDOS at the E_F for Hf_2SB, Hf_2SC, Hf_2SeB, Hf_2SeC, Hf_2TeB, and Hf_2TeC are 3.5, 1.60, 3.5, 1.8, 3.7, and 1.7 states per eV, respectively. Thus, the change in the A (A = S, Se, or Te)-site element does not significantly affect the DOS value at the E_F. However, the TDOS for the boride-based MAX phases is significantly higher compared with those of carbide-based MAX phases. Therefore, it is expected that the boride phase should exhibit higher electrical conductivity than the corresponding carbide counterpart.

For more theoretical understanding, the DOS of individual atoms Hf, A (S, Se, Te), and X (B, C) in the MAX phase structures are calculated and presented in Figure 3. The DOS curves have been shown from −10 to 5 eV in order to better comprehend the electronic states of each atom at various energy levels. The TDOS peaks at lower energy range from −10 to −2 eV are mainly contributed by Hf-*p*, Hf-*d*, S-*p*, and C-*p* states. The Hf-*p*, Hf-*d*, and B-*p* states are largely responsible for the emergence of DOS in the valance band near E_F (∼0 eV).

3.3. Thermal Properties. The MAX phase materials have the potential to be used in a variety of high-temperature technologies, including effective thermal barrier coatings, heating elements, and electrical connections.[8] Therefore, in order to reveal their uses in various high-temperature technologies, a thorough investigation of the thermodynamic characteristics of MAX phase materials is required. Consequently, fundamental thermodynamic parameters such as Debye temperature (Θ_D), minimum thermal conductivity (K_{min}), melting temperature (T_m), and Grüneisen parameter (γ) have been explored in this study for the Hf_2SB, Hf_2SC, Hf_2SeB, Hf_2SeC, Hf_2TeB, and Hf_2TeC MAX phases. The required equations for calculating Θ_D, T_m, K_{min}, and γ are embedded in the supporting section (eqs S16−S19). Previously, the thermodynamic properties of Hf_2SB,[14,20] Hf_2SC,[14,21] and Hf_2SeC[27] have been reported. As far as we are aware, there is still no information available about the thermodynamic properties of the Hf_2SeB, Hf_2TeB, and Hf_2TeC MAX phases.

https://doi.org/10.1021/acsomega.3c04283
ACS Omega 2023, 8, 32917−32930

Table 4. Calculated Crystal Density, Longitudinal, Transverse, and Average Sound Velocities (v_l, v_t, v_m), Debye Temperature Θ_D, Minimum Thermal Conductivity K_{min}, Grüneisen Parameter γ, and Melting Temperature T_m of Hf_2AX [A = S, Se, Te; X = B,C] MAX Phase Compounds

phases	ρ (g/cm^3)	v_l (m/s)	v_t (m/s)	v_m (m/s)	Θ_D (K)	K_{min} (W/mK)	γ	T_m (K)
Hf_2SB	10.196	5451	3299	3647	428	0.78	1.32	1656
ref 20					426			
ref 14	10.198	5465	3309	3657	430	0.79	1.32	1656
Hf_2SC	12.005	5643	3439	3799	470	0.90	1.28	1960
ref 14	10.192	5784	3431	3800	454	0.85	1.60	1778
ref 21	11.290	5820	3442	3813	463			
Hf_2SeB	10.805	4921	2870	3198	367	0.66	1.45	1461
Hf_2SeC	11.395	5185	3135	3465	406	0.74	1.32	1672
Hf_2TeB	10.797	4486	2600	2886	321	0.55	1.45	1264
Hf_2TeC	11.354	49 247	2923	3237	366	0.64	1.36	1540

The Debye temperature is connected to the lattice vibration, thermal expansion coefficient, specific heat, and melting point of the solid. It is termed as the maximum frequency mode of vibration in a solid. The calculation of Θ_D using elastic moduli is specified as one of the standard approaches.[55,56] The values of transverse sound velocity, v_t, longitudinal sound velocity, v_l, and averaged sound velocity, v_m, are used to estimate Θ_D using eq S16. The Θ_D of Hf_2TeC (366 K) is higher compared with that of Hf_2TeB (321 K), which is in good agreement with the elastic properties results. However, the Debye temperature of Hf_2TeC and Hf_2TeB is much lower than that of other Hf-based chalcogenide MAX phases, among which Hf_2SC exhibits the highest value of Θ_D. In the case of Hf-based phases, the Debye temperature usually lowers in value in spite of their higher elastic moduli, which might be due to the higher molecular mass of Hf. For example, Bouhemadou et al.[21] reported the Θ_D values of Ti_2SC, Zr_2SC, and Hf_2SC as 800, 603, and 463 K, respectively, whereas their elastic moduli are much closer in values.

The calculated values of ρ, v_t, v_l, v_m, Θ_D, K_{min}, γ, and T_m are listed in Table 4. The carbide phases have higher values of Θ_D compared with their boride counterparts as shown in Table 4.

The temperature at which a solid substance starts to melt is defined as melting temperature. Information on a material's melting temperature is necessary for high-temperature applications. The melting temperature is estimated using elastic constants (elastic constants C_{11} and C_{33} are connected to uniaxial stress) with the help of a well-known expression as presented in the supporting file (eq S17). The calculated T_m of Hf_2TeC is 3237 K, which is larger than Hf_2TeB (2886 K), due to the higher Young's modulus of Hf_2TeC (238 GPa) compared with Hf_2TeB (183 GPa). The knowledge of bonding strength can be known from the melting temperature because of its close relation with Young's modulus. Thus, a higher T_m is expected for a solid with a higher Y and vice versa.[57] A similar trend is also found for other chalcogenides presented here, in fact, it is also found in other systems, like Zr_2AB_2 (A = In, Tl).[57] However, among the investigated MAX phases, Hf_2SC has the highest melting temperature while Hf_2TeB has the lowest.

It is essential to disclose the ability of a material to conduct heat energy for thermal device applications. The knowledge of minimum thermal conductivity, K_{min}, is crucial for the high-temperature application of a material. Eq S18 was used to compute K_{min}. As evident from Table 4, the K_{min} of Hf_2TeC (0.64 W/mK) is higher than that of Hf_2TeB (0.55 W/mK). For application as a thermal barrier coating, a lower K_{min} is expected and from this perspective, Hf_2TeB might be more suitable than Hf_2TeC. But, other parameters, such as elastic moduli (bonding strength), Debye temperature, melting temperature, etc., suggest that Hf_2TeC should be more suitable for the high-temperature applications. A similar trend is also found for other boride and carbide phases considered here. The maximum value of K_{min} is observed for Hf_2SC and the minimum value for Hf_2TeB.

The Grüneisen parameter (γ) is a significant indicator for analyzing anharmonic effects within the crystal. It was calculated using the Poisson's ratio by using eq S19. According to Table 4, the estimated values of γ are seen to remain within the range of 0.85−3.53, as is typical for polycrystalline materials with the Poisson's ratio in the range of 0.05−0.46.[58] The present studied MAX phases exhibit low anharmonic effects as the values of γ close to the lower limit. It is also interesting to note that compared with their carbide counterparts, the boride phases exhibit a relatively higher anharmonic effect.

3.4. Optical Properties. The material response to incident photon energy and, consequently, electronic properties can be well understood by exploring the optical functions. The optical functions of Hf_2SB and Hf_2SC MAX phases have been studied earlier.[14] To the best of our survey, the optical functions of Hf_2SeB, Hf_2SeC, Hf_2TeB, and Hf_2TeC MAX phases still need to be explored. To ascertain whether these various carbide and boride MAX phases are appropriate for particular optical applications, this study thoroughly explores those. The macroscopic electronic response of a material can fully be described by the complex dielectric function, $\varepsilon(\omega) = \varepsilon_1(\omega) + i\varepsilon_2(\omega)$, where $\varepsilon_1(\omega)$ is the real part and $\varepsilon_2(\omega)$ is the imaginary part of the dielectric function. The imaginary part $\varepsilon_2(\omega)$ of the dielectric function can be expressed as[30,59]

$$\varepsilon_2(\omega) = \frac{2e^2\pi}{\Omega\varepsilon_0} \sum_{k,v,c} |\langle \psi_K^C | \hat{u}.\ \vec{r} | \psi_K^V \rangle|^2 \sigma(E_K^C - E_K^V - E)$$

where ω is the angular frequency of light, e is the electronic charge, $\hat{u}$ is the vector defining the polarization of the incident electric field, and ψ_K^C and ψ_K^V are the conduction and valence band wave functions at K, respectively. By using the Kramers−Kronig relations, the imaginary portion $\varepsilon_2(\omega)$ of the dielectric function can be used to deduce the real part $\varepsilon_1(\omega)$ of eq S21. The refractive index, absorption coefficient, loss function, reflectivity, and photoconductivity can be determined from $\varepsilon_1(\omega)$ and $\varepsilon_2(\omega)$ using eqs S22−S27.

https://doi.org/10.1021/acsomega.3c04283
ACS Omega 2023, 8, 32917−32930

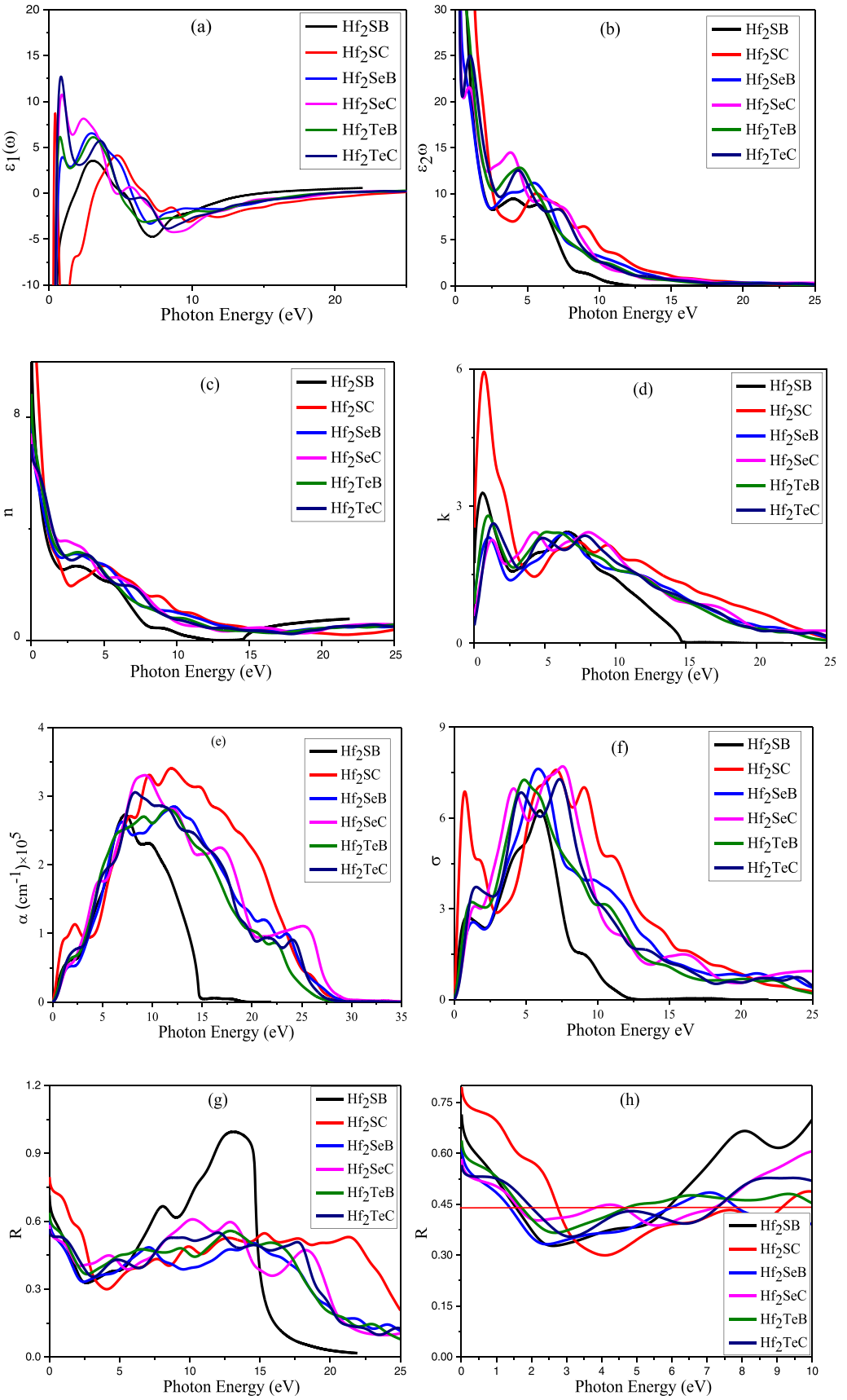

Figure 4. Calculated (a) real part, ε_1 of dielectric function, (b) imaginary part, ε_2 of dielectric function, (c) refractive index, n, (d) extinction coefficient, k, (e) absorption coefficient, α, (f) optical conductivity, σ, (g) reflectivity, R, and (g) low-energy part of R of Hf_2AX (A = S, Se, and Te; X = B, C) MAX phases as a function of photon energy.

https://doi.org/10.1021/acsomega.3c04283
ACS Omega 2023, 8, 32917−32930

Figure 4a,b displays the real (ε_1) and imaginary (ε_2) parts of dielectric functions, respectively. A high negative value of the real part of the dielectric functions and a high imaginary part's positive value of the dielectric function at zero energy are seen for all of the MAX phases, which is an expected behavior for a metallic system and consistent with the band structure results. The imaginary part of the dielectric function is directly associated with the optical absorption profile, and the imaginary part tends to have approximately zero value in the very high-energy region. The peaks in $\varepsilon_2(\omega)$ are associated with electron transitions, which might be intra-band transitions (inside M-*d* states) and/or inter-band transitions owing to photon absorption. Reaching zero value from below [real part, $\varepsilon_1(\omega)$] and above [imaginary part, $\varepsilon_2(\omega)$] is also another indication of the system's metallic nature. A similar pattern for the $\varepsilon_1(\omega)$ and $\varepsilon_2(\omega)$ of Ti_3SiC_2, the most widely studied MAX phase, is also reported.[60] The dielectric function of Cr_2GeC, Nb_2AlC, Ti_2AlC, Ti_2AlN, Ti_2SC, and Ti_3GeC_2 was also reported up to 5 eV, which also agrees well with the low-energy part of the present results.[61] The Hf_2SB shows the negligible value of the imaginary part above 12 eV, and all other MAX phases show above 20 eV, suggesting these MAX phases can be used as transparent materials in the high-energy region.

The refractive index, $n(\omega)$, and extinction coefficients, $k(\omega)$, of the studied MAX phases have been displayed in Figure 4c,d, respectively. The $n(\omega)$ regulates the propagation velocity of electromagnetic radiation through a material, whereas $k(\omega)$ determines the amount of radiation attenuation while traversing the material. The static values of $n(0)$ are 17.2, 11.7, 8.9, 8.4, 7.4, and 7.0 for Hf_2SC, Hf_2SB, Hf_2TeB, Hf_2SeB, Hf_2SeC, and Hf_2TeC. The static values of $n(0)$ for the studied MAX phases follow the same order with the static value of reflectivity at zero photon energy, i.e., Hf_2SC > Hf_2SB > Hf_2TeB > Hf_2SeB > Hf_2SeC > Hf_2TeC. The $k(\omega)$ curves are observed to vary approximately similarly to the $\varepsilon_2(\omega)$ as both of these parameters are related to the optical absorption.

Figure 4e shows the optical absorption profile of the studied MAX phases. The absorption coefficient (α) evaluates a material's incident energy-absorbing ability. A higher value of the absorption coefficient indicates a higher absorbing capability of the material and vice versa. From Figure 4e, we can notice that the optical absorption initiates at zero photon energy for all of the MAX compounds, which increases with increasing photon energy. The maximum absorption peaks for these MAX phases are noticed within 7−15 eV of photon energies, which indicates that these compounds are good candidates for effective absorbing materials within this energy range (ultraviolent region). The Hf_2TeC shows significantly higher optical absorption than its boride counterpart, Hf_2TeB, which is also true for other systems, i.e., the carbides have a higher absorption coefficient compared with their counterpart boride phases. The absorption nature is approximately similar for all carbide and boride counterparts except for a little difference in the spectra positions and heights of the peaks.

The optical conductivity reflects the results of optical absorption analysis. Figure 4f illustrates the optical conductivity profile of the studied MAX phases. Additionally, for all MAX phases, optical conductivity begins at zero photon energy, supporting the metallic character of all MAX compounds. This result strongly supports the optical absorption and electronic band structure calculations of the studied MAX phases. A notable optical conductivity peak is noticed in these MAX compounds' infrared to near-visible regions. Some other sharp conductivity peaks are also observed in the 5−10 eV of photon energies for all of the phases. All of the borides and carbides show approximately similar behavior with their corresponding counterpart, which also justifies the analysis of the optical absorption profile.

The reflectivity profile provides useful information about the suitability of a material as a reflector in a practical device. From Figure 4g, it can be observed that the reflectivity starts at zero photon energy with a value of 0.79, 0.71, 0.64, 0.62, 0.58, and 0.56 for Hf_2SC, Hf_2SB, Hf_2TeB, Hf_2SeB, Hf_2SeC, and Hf_2TeC MAX phases, respectively. According to Li et al.,[60] MAX phase materials with reflectivity greater than 44% can be used as coating materials to protect spaceships from solar heating. It is noted that the reflectivity spectra of Hf_2TeC exhibit a value higher than 44% up to 2.0 eV, while it is up to 1.85 eV for Hf_2TeB (marked by red line in Figure 4h). Thus, Hf_2TeC and Hf_2TeB MAX phases are also expected to be used for the above-mentioned applications, in which the IR part and low-energy part of visible rays are expected to be reflected back from the surface where it is covered by Hf_2TeC and Hf_2TeB's coating. As we know, the IR part of the solar radiation is mainly accountable for heat and heating surface. Like absorption coefficient and photoconductivity spectra, the carbide phases exhibit better reflectivity in the low-energy side compared with their counterpart's boride phases. However, the maximum reflectivity peak is observed at about 12 eV of photon energy for Hf_2SB as this boride phase shows lower absorption spectra near about this energy than other MAX phases. Very high reflectivity (above 90%) of Hf_2SB in the energy range from 11 to 14 eV in the ultraviolet (UV) region suggests that this particular MAX phase boride can also be used selectively as an excellent reflector in this range.

4. CONCLUSIONS

Using the DFT-based CASTEP code, the physical characteristics of the MAX phases Hf_2TeB and Hf_2TeC have been calculated and compared with those of Hf_2SB, Hf_2SC, Hf_2SeB, and Hf_2SeC. The Te-containing carbide MAX phase Hf_2TeC has been predicted for the first time in this study. The following concluding remarks can be made:

- The predicted MAX carbide phase (Hf_2TeC) is elastically and dynamically stable with negative formation energy.
- The investigation of lattice parameters, elastic constants, and elastic moduli of Hf_2SB, Hf_2SC, Hf_2SeB, Hf_2SeC, and Hf_2TeB reveals good consistency with previous reports.
- The elastic constants and moduli of Hf_2TeC are larger than those of Hf_2TeB. Hf_2SC is the stiffest, and the boride phase Hf_2TeB is the softest MAX phase among the investigated materials. The predicted carbide phase Hf_2TeC exhibits the highest value of machinability index (1.30) while the lowest value is found for Hf_2SC (1.09). The various anisotropy factors and direction-dependent elastic moduli revealed the anisotropic nature of all of the studied phases.
- The values of the melting temperature, minimum thermal conductivity, Grüneisen parameter, and Debye temperature suggest that Hf_2TeC is more suitable than Hf_2TeB for use in high-temperature technology; in fact, all carbide phases are more suitable than boride phases

https://doi.org/10.1021/acsomega.3c04283
ACS Omega 2023, 8, 32917−32930

for the same. The larger value of the elastic constants in the carbide phases compared with their boride counterparts may be the cause of this trend. The maximum value of melting temperature is found for Hf_2SC (1960 K) and the lowest value for Hf_2TeB (1264 K) among the studied MAX phases. All of the MAX phases have low anharmonic characters. The borides exhibit a higher anharmonic effect compared with their carbide counterparts.

- The study of optical functions, electronic band structure, and density of states ensures the metallic nature of all of the MAX phases under consideration. The reflectivity curve starts with 0.79, 0.71, 0.64, 0.62, 0.58, and 0.56 for Hf_2SC, Hf_2SB, Hf_2TeB, Hf_2SeB, Hf_2SeC, and Hf_2TeC MAX phases, respectively, at zero photon energy and remains high in the visible region. This reveals their appropriateness as coating materials to diminish solar heating. The carbide phases are expected to be more suitable than the borides.

The authors of this research article have high hopes that this work will aid in the designing of new MAX phase materials and exploring their intriguing features for applications in practical devices from different perspectives.

■ ASSOCIATED CONTENT

Supporting Information

The Supporting Information is available free of charge at https://pubs.acs.org/doi/10.1021/acsomega.3c04283.

Equations used to investigate various properties of Hf_2AX [A = S, Se, Te; X = B, C]; the crystallographic data of Hf_2SB; Mulliken atomic and bond overlap populations (BOP); anisotropy indices; theoretical wave numbers ω and symmetry assignment of the IR-active and Raman-active modes; electronic band structures of Hf_2AX [A = S, Se, Te; X = B, C] (PDF)

■ AUTHOR INFORMATION

Corresponding Authors

Md. Ashraf Ali − *Department of Physics, Chittagong University of Engineering and Technology (CUET), Chattogram 4349, Bangladesh; Advanced Computational Materials Research Laboratory, Department of Physics, Chittagong University of Engineering and Technology (CUET), Chattogram 4349, Bangladesh;* orcid.org/0000-0003-4957-2192; Email: ashrafphy31@cuet.ac.bd

Saleh Hasan Naqib − *Advanced Computational Materials Research Laboratory, Department of Physics, Chittagong University of Engineering and Technology (CUET), Chattogram 4349, Bangladesh; Department of Physics, University of Rajshahi, Rajshahi 6205, Bangladesh;* Email: salehnaqib@yahoo.com

Authors

Jakiul Islam − *Department of Physics, Noakhali Science and Technology University, Noakhali 3814, Bangladesh*

Md. Didarul Islam − *National Institute of Textile Engineering and Research, Dhaka 1350, Bangladesh;* orcid.org/0000-0002-4663-6624

Hasina Akter − *Department of Physics, Chittagong University of Engineering and Technology (CUET), Chattogram 4349, Bangladesh; Advanced Computational Materials Research Laboratory, Department of Physics, Chittagong University of Engineering and Technology (CUET), Chattogram 4349, Bangladesh*

Aslam Hossain − *National Institute of Textile Engineering and Research, Dhaka 1350, Bangladesh; Department of Physics, Chittagong University of Engineering and Technology (CUET), Chattogram 4349, Bangladesh*

Mautushi Biswas − *Department of Physics, Chittagong University of Engineering and Technology (CUET), Chattogram 4349, Bangladesh; Advanced Computational Materials Research Laboratory, Department of Physics, Chittagong University of Engineering and Technology (CUET), Chattogram 4349, Bangladesh*

Md. Mukter Hossain − *Department of Physics, Chittagong University of Engineering and Technology (CUET), Chattogram 4349, Bangladesh; Advanced Computational Materials Research Laboratory, Department of Physics, Chittagong University of Engineering and Technology (CUET), Chattogram 4349, Bangladesh;* orcid.org/0000-0003-2454-4996

Md. Mohi Uddin − *Department of Physics, Chittagong University of Engineering and Technology (CUET), Chattogram 4349, Bangladesh; Advanced Computational Materials Research Laboratory, Department of Physics, Chittagong University of Engineering and Technology (CUET), Chattogram 4349, Bangladesh;* orcid.org/0000-0001-7999-5079

Complete contact information is available at: https://pubs.acs.org/10.1021/acsomega.3c04283

Author Contributions

J.I.: Writing—original draft. M.D.I.: Writing—original draft. M.A.A.: Conceptualization, methodology, formal analysis, validation, project administration, writing—original draft, supervision. H.A.: Plotting figures, data calculations. A.H.: Plotting figures, data calculations. M.B.: Plotting figures, data calculations. M.M.H.: Writing—review and editing, validation. M.M.U.: Writing—review and editing, validation. S.H.N.: Formal analysis, writing—review and editing, validation.

Notes

The authors declare no competing financial interest.

■ ACKNOWLEDGMENTS

This work was carried out with the aid of a grant (grant number: 21−378 RG/PHYS/AS_G -FR3240319526) from UNESCO-TWAS and the Swedish International Development Cooperation Agency (SIDA). The views expressed herein do not necessarily represent those of UNESCO-TWAS, SIDA, or its Board of Governors.

■ REFERENCES

(1) Ali, M. A.; Qureshi, M. W. Newly Synthesized MAX Phase Zr2SeC: DFT Insights into Physical Properties towards Possible Applications. *RSC Adv.* **2021**, *11*, 16892−16905.

(2) Khatun, M. R.; Ali, M. A.; Parvin, F.; Islam, A. K. M. A. Elastic, Thermodynamic and Optical Behavior of V2AC (A = Al, Ga) MAX Phases. *Results Phys.* **2017**, *7*, 3634−3639.

(3) Lei, X.; Lin, N. Structure and Synthesis of MAX Phase Materials: A Brief Review. *Crit. Rev. Solid State Mater. Sci.* **2022**, *47*, 736−771.

(4) Surucu, G. Investigation of Structural, Electronic, Anisotropic Elastic, and Lattice Dynamical Properties of MAX Phases Borides: An Ab-Initio Study on Hypothetical M2AB (M = Ti, Zr, Hf; A = Al, Ga, In) Compounds. *Mater. Chem. Phys.* **2018**, *203*, 106−117.

(5) Ali, M. A.; Hossain, M. M.; Hossain, M. A.; Nasir, M. T.; Uddin, M. M.; Hasan, M. Z.; Islam, A.; Naqib, S. H. Recently Synthesized (Zr1-XTix) 2AlC (0 ≤ X ≤ 1) Solid Solutions: Theoretical Study of the Effects of M Mixing on Physical Properties. *J. Alloys Compd.* **2018**, *743*, 146−154.
(6) Ali, M. A.; Hossain, M. M.; Jahan, N.; Islam, A.; Naqib, S. H. Newly Synthesized Zr2AlC, Zr2(Al0.58Bi0.42)C, Zr2(Al0.2Sn0.8)C, and Zr2(Al0.3Sb0.7)C MAX Phases: A DFT Based First-Principles Study. *Comput. Mater. Sci.* **2017**, *131*, 139−145.
(7) Rackl, T.; Eisenburger, L.; Niklaus, R.; Johrendt, D. Syntheses and Physical Properties of the MAX Phase Boride Nb2SB and the Solid Solutions Nb2SBxC1-x(X = 0−1). *Phys. Rev. Mater.* **2019**, *3*, No. 054001.
(8) Gonzalez-Julian, J. Processing of MAX Phases: From Synthesis to Applications. *J. Am. Ceram. Soc.* **2021**, *104*, 659−690.
(9) Khazaei, M.; Arai, M.; Sasaki, T.; Estili, M.; Sakka, Y. Trends in Electronic Structures and Structural Properties of MAX Phases: A First-Principles Study on M2AlC(M = Sc, Ti, Cr, Zr, Nb, Mo, Hf, or Ta), M2AlN, and Hypothetical M2AlB Phases. *J. Phys.: Condens. Matter* **2014**, *26*, No. 505503.
(10) Zhao, S.; Chen, L.; Xiao, H.; Huang, J.; Li, Y.; Qian, Y.; Zheng, T.; Li, Y.; Cao, L.; Zhang, H.; Liu, H.; Wang, Y.; Huang, Q.; Wang, C. Phase Transformation and Amorphization Resistance in High-Entropy MAX Phase M2SnC (M = Ti, V, Nb, Zr, Hf) under in-Situ Ion Irradiation. *Acta Mater.* **2022**, *238*, No. 118222.
(11) Chen, L.; Li, Y.; Chen, K.; Bai, X.; Li, M.; Du, S.; Chai, Z.; Huang, Q. Synthesis and Characterization of Medium-/High-Entropy M2SnC (M = Ti/V/Nb/Zr/Hf) MAX Phases. *Small Struct.* **2023**, *4*, No. 2200161.
(12) Chen, K.; Chen, Y.; Zhang, J.; Song, Y.; Zhou, X.; Li, M.; Fan, X.; Zhou, J.; Huang, Q. Medium-Entropy (Ti, Zr, Hf)2SC MAX Phase. *Ceram. Int.* **2021**, *47*, 7582−7587.
(13) Xiong, K.; Sun, Z.; Zhang, S.; Wang, Y.; Li, W.; You, L.; Yang, L.; Guo, L.; Mao, Y. A Comparative Study the Structural, Mechanical, and Electronic Properties of Medium-Entropy MAX Phase (TiZrHf)-2SC with Ti2SC, Zr2SC, Hf2SC via First-Principles. *J. Mater. Res. Technol.* **2022**, *19*, 2717−2729.
(14) Ali, M. A.; Hossain, M. M.; Uddin, M. M.; Hossain, M. A.; Islam, A. K. M. A.; Naqib, S. H. Physical Properties of New MAX Phase Borides M2SB (M = Zr, Hf and Nb) in Comparison with Conventional MAX Phase Carbides M2SC (M = Zr, Hf and Nb): Comprehensive Insights. *J. Mater. Res. Technol.* **2021**, *11*, 1000−1018.
(15) Hossein-Zadeh, M.; Ghasali, E.; Mirzaee, O.; Mohammadian-Semnani, H.; Alizadeh, M.; Orooji, Y.; Ebadzadeh, T. An Investigation into the Microstructure and Mechanical Properties of V2AlC MAX Phase Prepared by Microwave Sintering. *J. Alloys Compd.* **2019**, *795*, 291−303.
(16) Sharma, P.; Singh, K.; Pandey, O. P. Investigation on Oxidation Stability of V2AlC MAX Phase. *Thermochim. Acta* **2021**, *704*, No. 179010.
(17) Lu, Y.; Khazaei, M.; Hu, X.; Khaledialidusti, R.; Sasase, M.; Wu, J.; Hosono, H. Facile Synthesis of Ti2AC (A = Zn, Al, In, and Ga) MAX Phases by Hydrogen Incorporation into Crystallographic Voids. *J. Phys. Chem. Lett.* **2021**, *12*, 11245−11251.
(18) Cabioch, T.; Eklund, P.; Mauchamp, V.; Jaouen, M.; Barsoum, M. W. Tailoring of the Thermal Expansion of Cr2 (Alx, Ge1−x)C Phases. *J. Eur. Ceram. Soc.* **2013**, *33*, 897−904.
(19) Li, Y.; Lu, J.; Li, M.; Chang, K.; Zha, X.; Zhang, Y.; Chen, K.; Persson, P. O.; et al. Multielemental single−atom-thick A layers in nanolaminated V2 (Sn, A) C (A= Fe, Co, Ni, Mn) for tailoring magnetic properties. *Proc. Natl. Acad. Sci.* **2020**, *117*, 820−825.
(20) Rackl, T.; Johrendt, D. The MAX Phase Borides Zr2SB and Hf2SB. *Solid State Sci.* **2020**, *106*, No. 106316.
(21) Bouhemadou, A.; Khenata, R. Structural, Electronic and Elastic Properties of M2SC (M = Ti, Zr, Hf) Compounds. *Phys. Lett. A* **2008**, *372*, 6448−6452.
(22) Wang, X.; Chen, K.; Wu, E.; Zhang, Y.; Ding, H.; Qiu, N.; Song, Y.; Du, S.; Chai, Z.; Huang, Q. Synthesis and Thermal Expansion of Chalcogenide MAX Phase Hf2SeC. *J. Eur. Ceram. Soc.* **2022**, *42*, 2084−2088.
(23) Zhang, Q.; Zhou, Y.; et al. Zr2SeB and Hf2SeB: Two New MAB Phase Compounds with the Cr2AlC-Type MAX Phase (211 Phase) Structure. *J. Adv. Ceram.* **2022**, *11*, 1764−1776.
(24) Zhang, Q.; Zhou, Y.; San, X.; Li, W.; Bao, Y.; Feng, Q.; Grasso, S.; Hu, C. Zr2SeB and Hf2SeB: Two New MAB Phase Compounds with the Cr2AlC-Type MAX Phase (211 Phase) Crystal Structures. *J. Adv. Ceram.* **2022**, *11*, 1764−1776.
(25) Zhang, Q.; Zhou, Y.; San, X.; Wan, D.; Bao, Y.; Feng, Q.; Grasso, S.; Hu, C. Thermal Explosion Synthesis of First Te-Containing Layered Ternary Hf2TeB MAX Phase. *J. Eur. Ceram. Soc.* **2023**, *43*, 173−176.
(26) Zhou, Y.; Xiang, H.; Hu, C. Extension of MAX Phases from Ternary Carbides and Nitrides (X = C and N) to Ternary Borides (X = B, C, and N): A General Guideline. *Int. J. Appl. Ceram. Technol.* **2023**, *20*, 803−822.
(27) Ali, M. A.; Waqas, M. DFT Insights into the New Hf-Based Chalcogenide MAX Phase Hf2SeC. *Vacuum* **2022**, *201*, No. 111072.
(28) Hohenberg, P.; Kohn, W. Inhomogeneous Electron Gas. *Phys. Rev.* **1964**, *136*, No. B864.
(29) Kohn, W.; Sham, L. J. Self-Consistent Equations Including Exchange and Correlation Effects. *Phys. Rev.* **1965**, *140*, A1133.
(30) Clark, S. J.; Segall, M. D.; Pickard, C. J.; Hasnip, P. J.; Probert, M. I. J.; Refson, K.; Payne, M. C. First Principles Methods Using CASTEP. *Z. Kristallogr. - Cryst. Mater.* **2005**, *220*, 567−570.
(31) Perdew, J. P.; Burke, K.; Ernzerhof, M. Generalized Gradient Approximation Made Simple. *Phys. Rev. Lett.* **1996**, *77*, 3865.
(32) Vanderbilt, D. Soft Self-Consistent Pseudopotentials in a Generalized Eigenvalue Formalism. *Phys. Rev. B* **1990**, *41*, 7892.
(33) Fischer, T. H.; Almlof, J. General Methods for Geometry and Wave Function Optimization. *J. Phys. Chem. A* **1992**, *96*, 9768−9774.
(34) Monkhorst, H. J.; Pack, J. D. Special Points for Brillouin-Zone Integrations. *Phys. Rev. B* **1976**, *13*, 5188.
(35) Born, M.On the Stability of Crystal Lattices. I. In *Mathematical Proceedings of the Cambridge Philosophical Society*; Cambridge University Press, 1940; Vol. *36*, pp 160−172 DOI: 10.1017/S0305004100017138.
(36) Chowdhury, A.; Ali, M. A.; Hossain, M. M.; Uddin, M. M.; Naqib, S. H.; Islam, A. K. Predicted MAX Phase Sc2InC: Dynamical Stability, Vibrational and Optical Properties. *Phys. Status Solidi* **2018**, *255*, No. 1700235.
(37) Yang, Y.; Wang, J.; Liu, Y.; Cui, Y.; Ding, G.; Wang, X. Topological Phonons in Cs-Te Binary Systems. *Phys. Rev. B* **2023**, *107*, 24304.
(38) Yang, Y.; Xie, C.; Cui, Y.; Wang, X.; Wu, W. Maximally Charged Single-Pair Multi-Weyl Point Phonons in P23-Type BeH2. *Phys. Rev. B* **2023**, *107*, 54310.
(39) Ding, G.; Wang, J.; Yu, Z.-M.; Zhang, Z.; Wang, W.; Wang, X. Single Pair of Type-III Weyl Points Half-Metals: BaNiIO6 as an Example. *Phys. Rev. Mater.* **2023**, *7*, 14202.
(40) Ali, M. A.; Nasir, M. T.; et al. An Ab Initio Investigation of Vibrational, Thermodynamic, and Optical Properties of Sc2AlC MAX Compound. *Chin. Phys. B* **2016**, *25*, No. 103102.
(41) Hadi, M. A.; Christopoulos, S. R.; Chroneos, A.; Naqib, S. H.; Islam, A. K. DFT Insights into the Electronic Structure, Mechanical Behaviour, Lattice Dynamics and Defect Processes in the First Sc-Based MAX Phase Sc2SnC. *Sci. Rep.* **2022**, *12*, No. 14037.
(42) Champagne, A.; Bourdarot, F.; Bourges, P.; Piekarz, P.; Pinek, D.; Gélard, I.; Charlier, J.-C.; Ouisse, T. Phonon Dispersion Curves in Cr2AlC Single-Crystals. *Mater. Res. Lett.* **2018**, *6*, 378−383.
(43) Aydin, S.; Tatar, A.; Ciftci, Y. O. Some New Members of MAX Family Including Light-Elements: Nanolayered Hf2XY (X = Al, Si, P and YCombining Double Low LineB, C, N). *Solid State Sci.* **2016**, *53*, 44−55.
(44) Zhang, H.; Tang, Y.; Zhong, X.; Zhang, Y.; Song, H.; Wang, J.; Wang, Q. The Electronic, Elastic and Thermodynamic Properties of Carbon- and Nitrogen-Doped Hf2PB: A Theoretical Approach. *Mater. Res. Express* **2019**, *6*, No. 056507.

https://doi.org/10.1021/acsomega.3c04283
ACS Omega 2023, 8, 32917−32930

(45) Pettifor, D. G. Theoretical Predictions of Structure and Related Properties of Intermetallics. *Mater. Sci. Technol.* **1992**, *8*, 345−349.
(46) Voigt, W. *Lehrbuch Der Kristallphysik: Teubner-Leipzig* 1928.
(47) Hill, R. The Elastic Behaviour of a Crystalline Aggregate. *Proc. Phys. Soc. Sect. A* **1952**, *65*, 349.
(48) Bouhemadou, A. First-Principles Study of Structural, Electronic and Elastic Properties of Nb4AlC3. *Braz. J. Phys.* **2010**, *40*, 52−57.
(49) Islam, J.; Hossain, A. A. Narrowing Band Gap and Enhanced Visible-Light Absorption of Metal-Doped Non-Toxic CsSnCl3 Metal Halides for Potential Optoelectronic Applications. *RSC Adv.* **2020**, *10*, 7817−7827.
(50) Sun, Z.; Music, D.; Ahuja, R.; Schneider, J. M. Theoretical Investigation of the Bonding and Elastic Properties of Nanolayered Ternary Nitrides. *Phys. Rev. B* **2005**, *71*, No. 193402.
(51) Pugh, S. F. XCII. Relations between the Elastic Moduli and the Plastic Properties of Polycrystalline Pure Metals. *London, Edinburgh, Dublin Philos. Mag. J. Sci.* **1954**, *45*, 823−843.
(52) Frantsevich, I. N.; Voronov, F. F.; Bakuta, S. A.Handbook on Elastic Constants and Moduli of Elasticity for Metals and Nonmetals *Kiev: Naukova Dumka* 1982.
(53) Sultana, F.; Uddin, M. M.; Ali, M. A.; Hossain, M. M.; Naqib, S. H.; Islam, A. K. M. A. First Principles Study of M2InC (M = Zr, Hf and Ta) MAX Phases: The Effect of M Atomic Species. *Results Phys.* **2018**, *11*, 869−876.
(54) Ali, M. A.; Naqib, S. H. Recently Synthesized (Ti1−xMox)2AlC (0 ≤ x ≤ 0.20) Solid Solutions: Deciphering the Structural, Electronic, Mechanical and Thermodynamic Properties via Ab Initio Simulations. *RSC Adv.* **2020**, *10*, 31535−31546.
(55) Anderson, O. L. A Simplified Method for Calculating the Debye Temperature from Elastic Constants. *J. Phys. Chem. Solids* **1963**, *24*, 909−917.
(56) Islam, J.; Hossain, A. K. M. A. Investigation of Physical and Superconducting Properties of Newly Synthesized CaPd2P2 and SrPd2P2. *J. Alloys Compd.* **2021**, *868*, No. 159199.
(57) Ali, M. A.; Hossain, M. M.; Uddin, M. M.; Islam, A. K. M. A.; Naqib, S. H. Understanding the Improvement of Thermo- Mechanical and Optical Properties of 212 MAX Phase Borides Zr2AB2(A = In, Tl). *J. Mater. Res. Technol.* **2021**, *15*, 2227−2241.
(58) Mikitishin, S. I. Interrelationship of Poisson's Ratio with Other Characteristics of Pure Metals. *Soviet materials science: a transl. of Fiziko-khimicheskaya mekhanika materialov/Academy of Sciences of the Ukrainian SSR* **1982**, *18*, 262−265.
(59) Naher, M. I.; Naqib, S. H. An Ab-Initio Study on Structural, Elastic, Electronic, Bonding, Thermal, and Optical Properties of Topological Weyl Semimetal TaX (X = P, As). *Sci. Rep.* **2021**, *11*, No. 5592.
(60) Li, S.; Ahuja, R.; Barsoum, M. W.; Jena, P.; Johansson, B. Optical Properties of Ti3SiC2 and Ti4AlN3. *Appl. Phys. Lett.* **2008**, *92*, No. 221907.
(61) Rybka, M. *Optical Properties of MAX-Phase Materials: Linköping University* 2010.

https://doi.org/10.1021/acsomega.3c04283
ACS Omega 2023, 8, 32917−32930